Supporting Material

Macromolecular crowding effects on two homologs of ribosomal protein S16:
Protein-dependent structural changes and local interactions

Therese Mikaelsson, Jörgen Ådén, Pernilla Wittung-Stafshede* and Lennart B.-Å. Johansson*

Department of Chemistry, Umeå University, 90187 Umeå, Sweden

*Corresponding authors: lennart.johansson@chem.umu.se; pernilla.wittung@chem.umu.se

Content:

Tables S1-S3
Figures S1-S5

Table S1 Effects of dextran 20 on $S16_{Meso}$ WT thermodynamic stability, measured at three fixed different temperatures using urea-induced denaturation.

Temperature (°C)	Buffer $\Delta G°_u$ (kJ mol^{-1})	Dextran 20 (200 mg/mL) $\Delta G°_u$ (kJ mol^{-1})	$\ln (K_{u\,crowd}/K_{u\,buff})$*
10	9.8 ± 0.7	12.2 ± 1.1	1.0
25	14.0 ± 1.0	15.1 ± 1.2	0.5
40	9.4 ± 1.8	12.1 ± 2.0	1.0

* $\ln K_u = -\Delta G°_u/RT$

Table S2 Quantum yields and average fluorescence lifetimes of BODIPY .

[Dextran] (mg/mL)	**W74F/F10C**		**W74C**		**W39F/Q10C**		**W39F/K74C**		**W39F/Y81C**	
	$\boldsymbol{\phi}$	$\langle\boldsymbol{\tau}\rangle$ **(ns)**	$\boldsymbol{\phi}$	$\langle\boldsymbol{\tau}\rangle$ **(ns)**	$\boldsymbol{\phi}$	$\langle\boldsymbol{\tau}\rangle$ **(ns)**	$\boldsymbol{\phi}$	$\langle\boldsymbol{\tau}\rangle$ **(ns)**	$\boldsymbol{\phi}$	$\langle\boldsymbol{\tau}\rangle$ **(ns)**
0	0.66	5.9	1.04	6.1	1.00	6.2	1.10	6.0	0.30	6.1
50	0.57	5.8	0.97	6.1	0.98	6.1	0.93	6.0	0.33	6.1
100	0.51	5.8	0.82	6.1	0.97	6.1	1.09	6.0	0.27	6.0
200	0.52	5.7	0.62	5.9	0.91	6.0	0.90	5.9	0.30	5.9
300	0.58	5.6	0.79	5.9	0.76	5.9	0.97	5.9	0.27	5.8

The quantum yield ($\boldsymbol{\phi}$) together with the average fluorescence lifetime ($\langle\boldsymbol{\tau}\rangle$) of BODIPY for the two $S16_{Thermo}$ variants; W74C/F10C and W74C and three $S16_{Meso}$ variants; W39F/Q10C, W39F/K74C and W39F/Y81C. Measurements were performed at different concentrations of dextran 20. The errors of the quantum yield measurements are within 10 %.

Table S3 Quantum yields and fluorescence lifetimes of BODIPY at different dextran concentrations.

[Dextran] (mg/mL)	W39F/K74C						W39F/Q10C					
	Dextran			Tyr-dextran			Dextran			Tyr-dextran		
	ϕ	$\langle\tau\rangle$ (ns)	τ_{long} (ns)	ϕ	$\langle\tau\rangle$ (ns)	τ_{long} (ns)	ϕ	$\langle\tau\rangle$ (ns)	τ_{long} (ns)	ϕ	$\langle\tau\rangle$ (ns)	τ_{long} (ns)
0	1.01	6.0	6.0	1.01	6.0	6.0	0.99	5.9	6.2	0.99	5.9	6.2
50	1.02	6.0	6.0	0.96	5.7	5.8	0.98	5.8	6.0	0.72	5.5	5.8
100	1.02	6.0	6.0	0.93	5.5	5.6	1.01	5.8	6.0	0.74	5.3	5.6
150	1.00	6.0	6.0	0.88	5.4	5.5	1.03	5.8	6.0	0.76	5.3	5.6

[Dextran] (mg/mL)	W74C								
	Dextran			Tyr-dextran			1.5 mM Tyr		
	ϕ	$\langle\tau\rangle$ (ns)	τ_{long} (ns)	ϕ	$\langle\tau\rangle$ (ns)	τ_{long} (ns)	ϕ	$\langle\tau\rangle$ (ns)	τ_{long} (ns)
0	0.96	6.2	6.2	0.96	6.2	6.2	0.98	6.0	6.1
12.5	-	-	-	0.56	5.3	5.9	-	-	-
25	-	-	-	0.44	5.0	5.9	-	-	-
50	0.90	6.1	6.1	0.54	5.3	5.9	0.93	5.9	6.0
75	-	-	-	0.74	5.6	5.8	-	-	-
100	0.82	6.1	6.1	0.86	5.8	5.9	-	-	-
150	0.80	6.0	6.1	0.82	5.7	5.9	-	-	-

The quantum yield (ϕ) together with the average fluorescence lifetime ($\langle\tau\rangle$) and the long component lifetime (τ_{long}) analysed between 10 – 30 ns, for the two $S16_{Meso}$ variants W39F/K74C and W39F/Q10C as well as the $S16_{Thermo}$ mutant W74C. Measurements were performed at varying concentrations of dextran 20 and the tyrosine labelled dextran (Tyr-dextran). The errors of the quantum yield measurements are within 10 %. Also shown are the control data for W74C-BODIPY in presence of 1.5 mM free tyrosine.

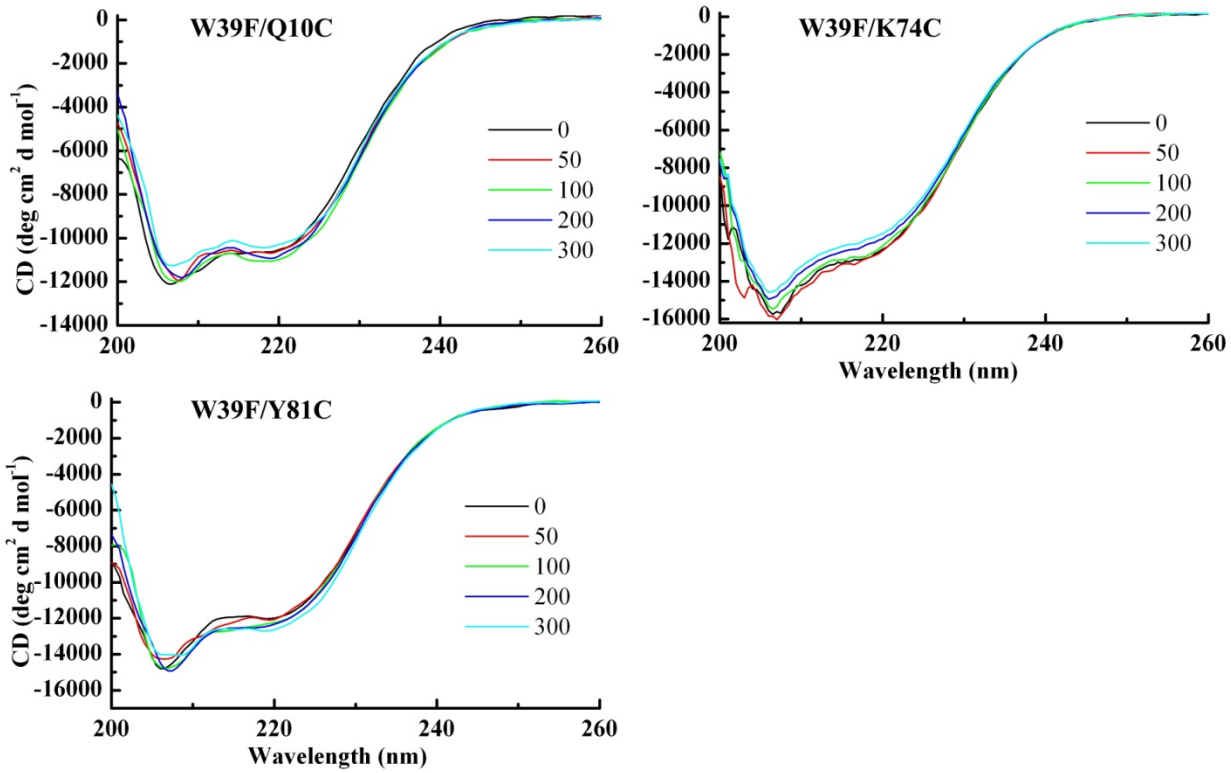

Figure S1. Far-UV CD spectra of the three $S16_{Meso}$ mutants at varying concentrations of dextran 20 (given in mg/mL in the panels with colour codes).

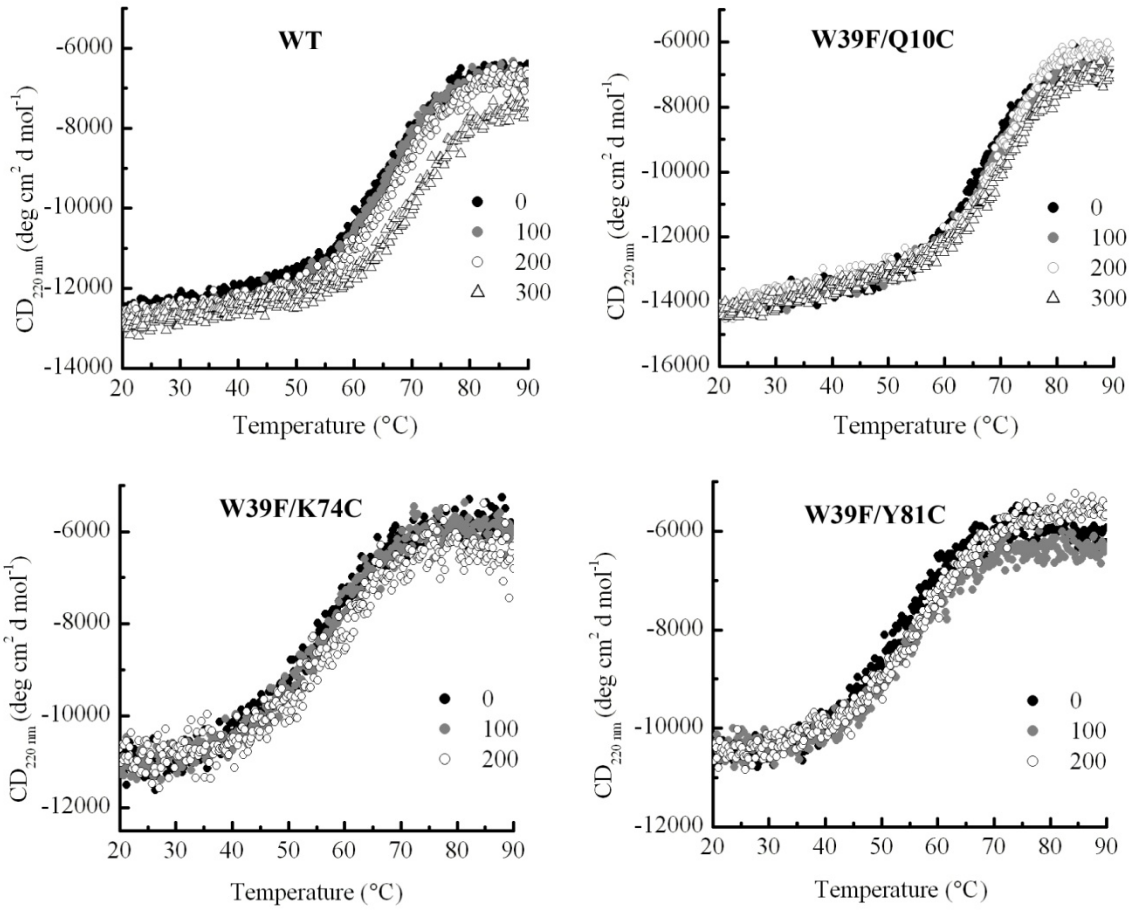

Figure S2. Thermal unfolding of $S16_{Meso}$, at varying amounts of dextran 20 for wild-type (WT) and the three mutants W39F/Q10C, W39F/K74C and W39F/Y81C (amount of dextran 20 in mg/ml is given in the panels). The reversibility of unfolding was confirmed by the return of the negative CD signal at 220 nm after cooling. All thermal curves shown were reversible.

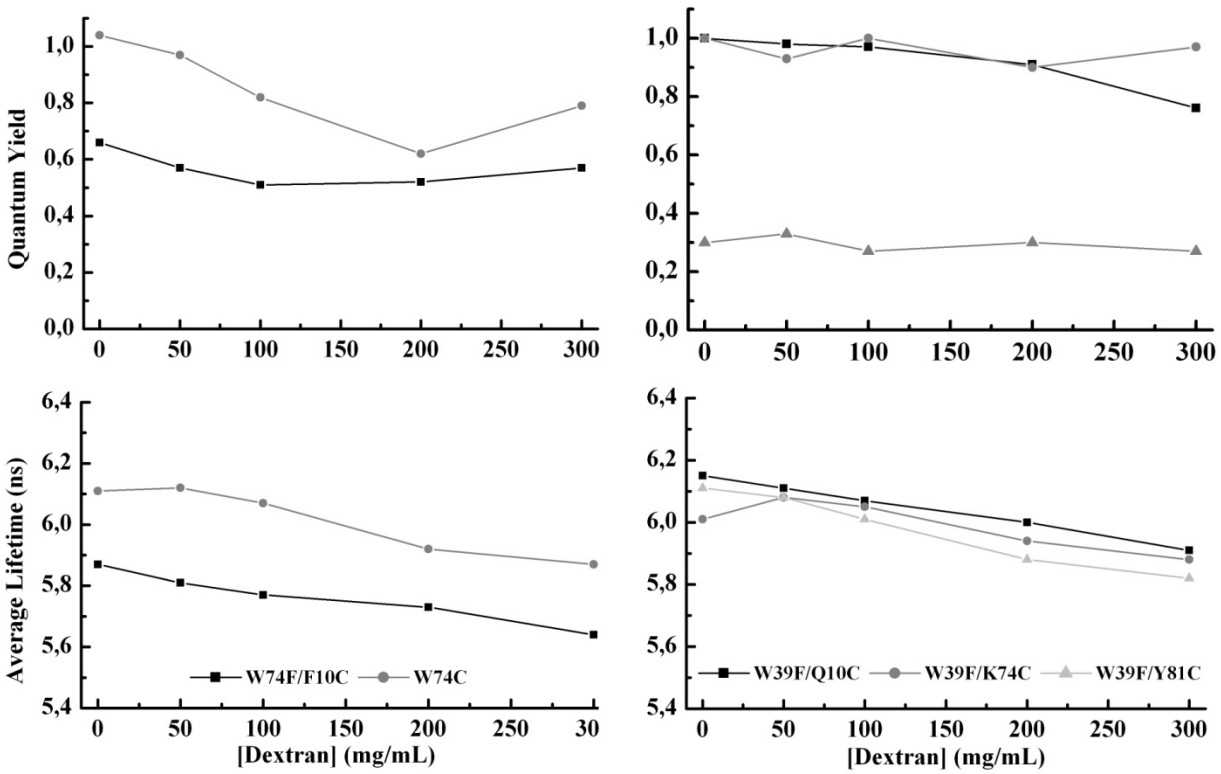

Figure S3 Quantum yield (*upper panels*) and average fluorescence lifetimes (*lower panels*) of BODIPY in the two $S16_{Thermo}$ (*left panels*) and three $S16_{Meso}$ (*right panels*) variants at varying concentrations of dextran 20.

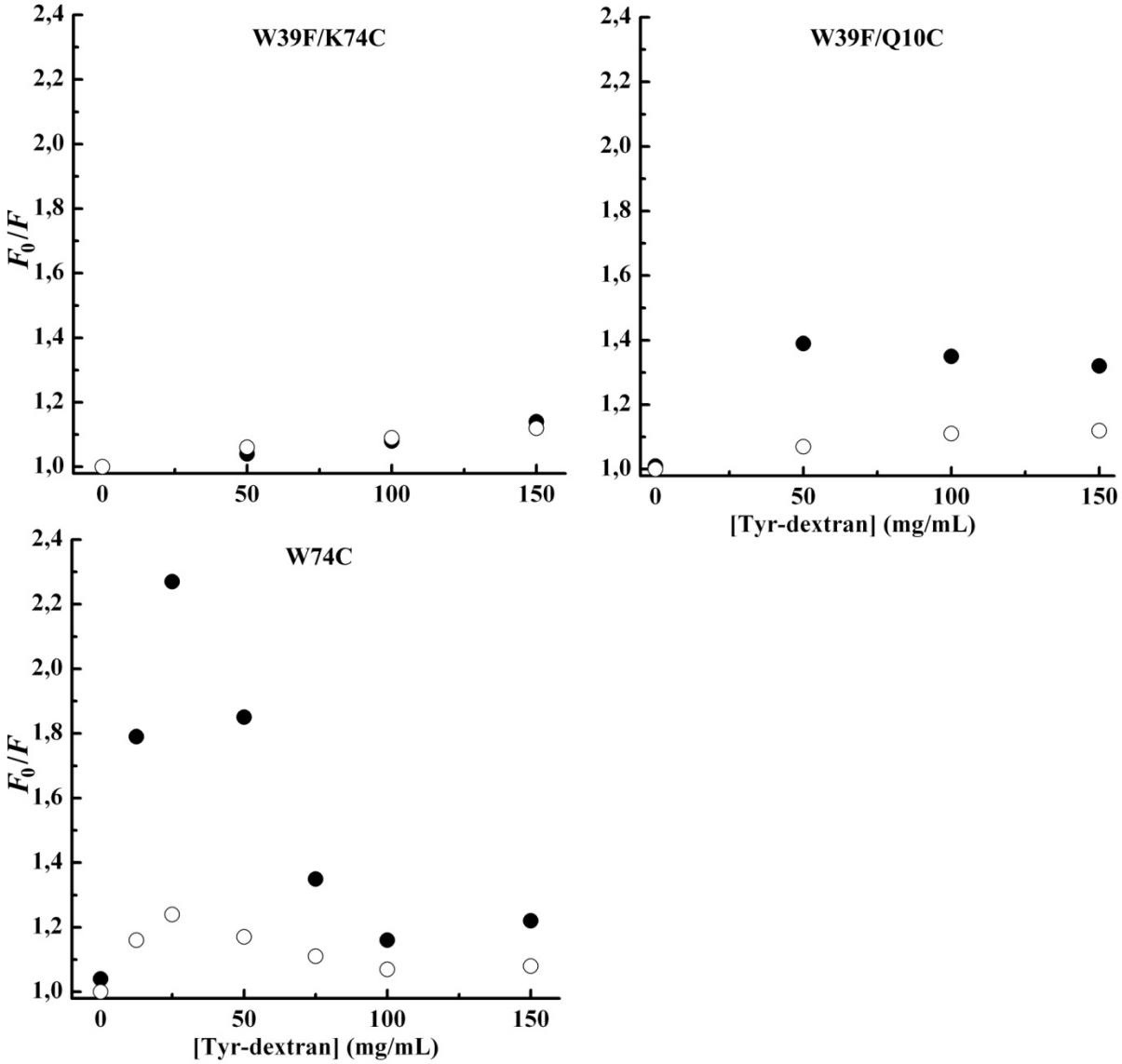

Figure S4. Stern-Volmer plots for three of the S16 variants, where the fluorescence intensity ratio F_0/F shows how ϕ_0/ϕ (o) and τ_0/τ (●) varies with the tyrosine-labelled dextran concentration.

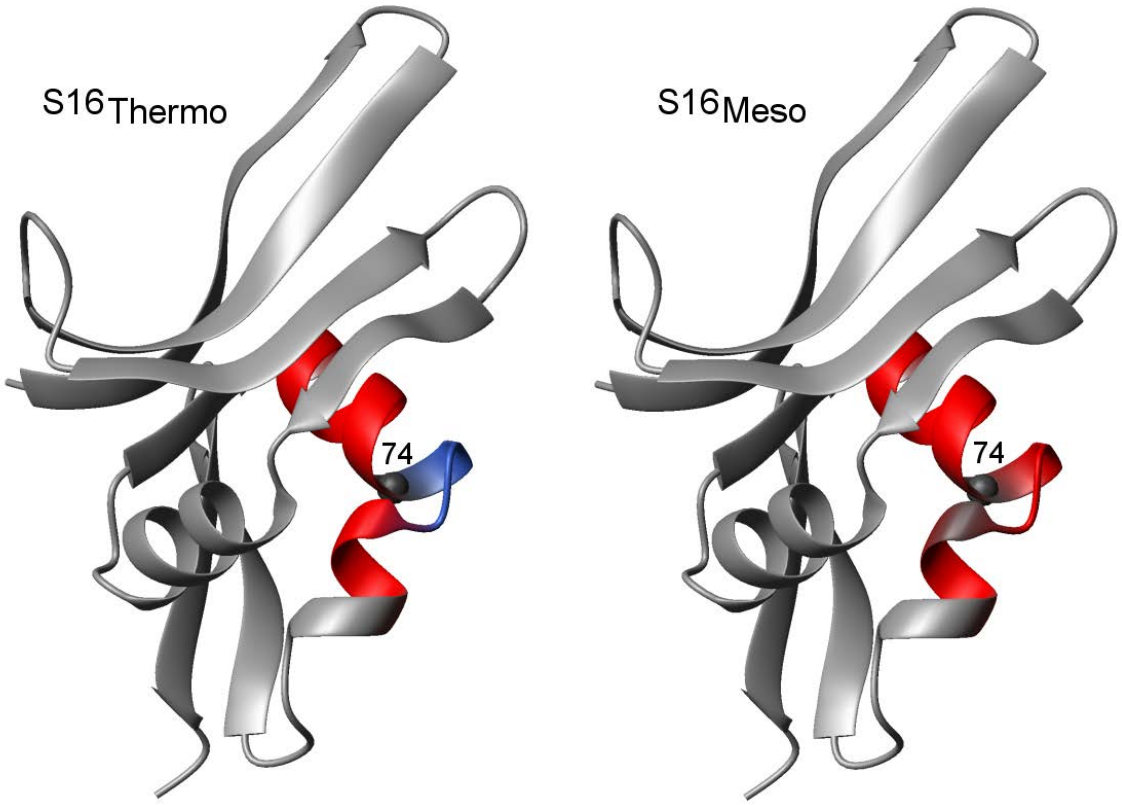

Figure S5. Sequential HN-HN NOE (Nuclear Overhauser Effect) contacts observed for residues 68 to 80 (Wallgren, M. et al., Journal of Molecular Biology, 2008. **379**(4): p. 845-858) plotted for both S16 homologs. Strong contacts are marked in red. The Cα atom for residue 74 is shown as a grey sphere. Residues 74-76 show strong inter-NOE contacts for $S16_{Meso}$ but not in $S16_{Thermo}$ (blue) as indicated in the figure.